

Experimental and Numerical Study on Flexural Structural Reinforced Concrete Walls under High Axial Load

NETRATTANA Chanipa¹, TAKAHASHI Tatsuya², OBARA Taku³, KONO Susumu⁴, MUKAI David⁵

¹PhD candidate, Tokyo Institute of Technology, netrattana.c.aa@m.titech.ac.jp

²Graduate student, Tokyo Institute of Technology, takahashi.t.ce@m.titech.ac.jp

³Assistant professor, Tokyo Institute of Technology, obara.t.ac@m.titech.ac.jp

⁴Professor, Tokyo Institute of Technology, kono.s.ae@m.titech.ac.jp

⁵Associate professor, University of Wyoming, dmukai@uwyo.edu

Abstract— An experiment was conducted on two 1/3 scale slender rectangular RC walls to study effect of 20% and 40% axial load ratio on their seismic performance. A fiber cross-section based model was used to simulate lateral load-drift response and assess characteristic points: flexural crack, yield of vertical reinforcement, peak load and ultimate deformation. Through the experimental results, axial load ratio of 40% has a detrimental effect on dramatically decreasing ultimate deformation and immediately collapse due to concrete crushing. The model could capture lateral load-drift response and all characteristic points accurately. Ultimate deformation was well estimated by hoop rebar strain of 0.2% which was obtained from experiment near collapse point.

I. INTRODUCTION

After the 2010 Maule Chile Earthquake, damages that mainly observed in slender reinforced concrete wall were concrete crushing and reinforcement rebar buckling at wall boundary [1]. A study from Massone et al. [2] revealed that post-1985 Chilean buildings, and particularly buildings constructed after 2000, taller buildings, tended to have axial force ratios, typically in the range of 10% to 30% of cross-section capacity, and sometimes larger for individual walls.

This study presents the results of an experimental and numerical study of two slender rectangular reinforced concrete walls under axial load ratio of 20% and 40%.

II. EXPERIMENTAL SET UP

An experiment was conducted on two 1/3 scale slender rectangular RC walls with confinement at boundary regions to study effect of high axial load ratio on their seismic performance. These two identical specimens were subjected to constant 20% and 40% axial load ratio. Summary of specimen properties is shown in Table 1. Specimen geometry, reinforcement detailing and strain gauge location in vertical rebar and hoop bar is shown in Fig 1.

III. EXPERIMENTAL RESULTS

Fig. 2 shows experimental lateral load-drift relation of RC walls under 20% and 40% axial load ratio. This figure also shows characteristic points: flexural crack, yield of vertical reinforcement, maximum load and ultimate point. Flexural crack initiated at 0.14% drift for RW20, while 0.26% for RW40. First flexural crack of RW40 was delayed due to high

axial compressive stress. Vertical reinforcement at end region yield in compression at 0.4% drift for RW20, while 0.09% drift for RW40. RW20 and RW40 reached maximum lateral load of 161.0 kN and 214.4 kN, respectively. After maximum load, lateral load of RW40 decreased dramatically until concrete exploded and out-of-plane instability occurred. Lateral load of RW20 decreased gradually until core concrete crushing and out-of-plane instability.

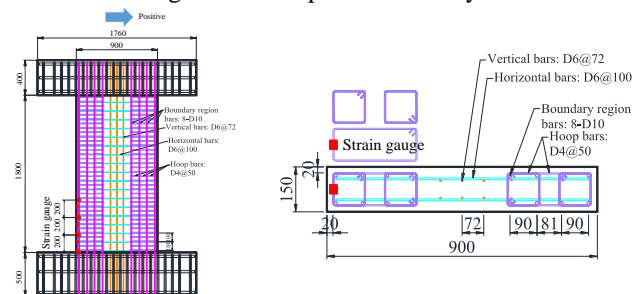


Fig.1 Specimen properties

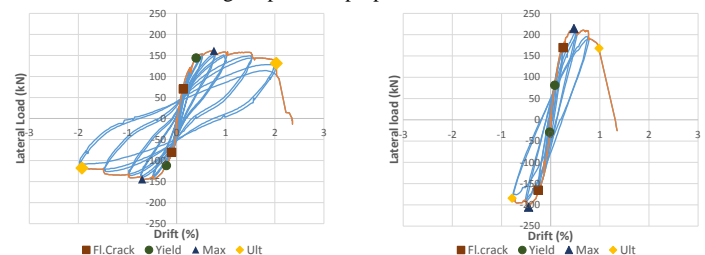


Fig.2 Lateral load-drift relation and characteristics points

Table 1 Specimen properties

Specimen	Parameter	lw (mm)	hu (mm)	tw (mm)	Confined Area				Wall Panel		Axial load ratio	Shear Span Ratio
					Vert. rebar		Confinement rebar		Vert. rebar	Hor. rebar		
					Arrange	ρ_v (%)	Arrange	ρ_s (%)				
RW20	Bench Mark	900	1800	150	8D10	1.84	D4@50	1.29	2-D6@72	2-D6@100	0.2	3.33
RW40	Axial load								0.4			

Note: lw: wall length, hu: wall height, tw: wall thickness, ρ_v : vertical rebar area ratio, ρ_s : volumetric confined rebar ratio

IV. ANALYTICAL MODEL

A. Simulation of lateral load-drift relation

Lateral load-drift relations were evaluated based on fiber cross-section as shown in Fig 3. Effects of confinement are taken into account by modelling the concrete inside the hoop rebar with confined concrete model [3]. The remaining concrete is modelled as plain concrete. The cyclic response of concrete was defined using Kent and Park model [4] and Karsan-Jirsa [5]. Tensile strength of concrete was neglected. The cyclic response of reinforcing steel was defined using Giuffre-Menegotto-Pinto model [6]

In order to determine flexural deformation, curvature was assumed as shown in Fig. 4. Plastic curvature distributed constant over plastic hinge length. In this study, plastic hinge length equaled to 0.3 of wall length. Shear deformation was approximated by Beyer et al. [7].

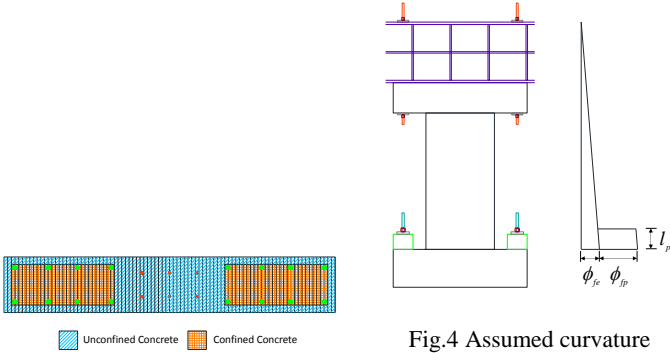


Fig.4 Assumed curvature distribution

B. Ultimate deformation

Ultimate deformation was determined when extreme confined concrete fiber reached ultimate confined concrete compressive strain. The ultimate confined concrete compressive strain, ε_{cu} , was estimated by Mander et al. [7] as shown in Eq. 1. Concept of ultimate point was when hoop rebar fracture, thus originally defined as fracture strain of hoop rebar. However, fracture of hoop rebar was not observed in this experiment. In this study, hoop rebar strain were obtained experimentally 0.2% and 0.4% for RC walls under 20% and 40% axial load ratio, respectively. Hoop rebar strain of 0.2% was used for conservative estimation.

$$\varepsilon_{cu} = 0.004 + 1.4\rho_s f_{yh} \varepsilon_{sm} / f'_{cc} \quad (1)$$

where ρ_s : volumetric confinement rebar ratio, f_{yh} : confined rebar yield strength, ε_{sm} : measured peak hoop rebar strain, f'_{cc} : confined concrete strength

V. ANALYSIS RESULTS

The results show that the model is able to capture lateral load-drift relation of RC walls under 20% and 40% axial load ratio. All characteristic points starting from flexural crack point, vertical reinforcement yield point, maximum load point and ultimate point could be assessed by this model. Lateral load of RW40 slightly overestimated. Ultimate deformations of both walls were well predicted by 0.2% hoop rebar strain assumption. Load capacity at ultimate point overestimate for both walls. For this issue, degradation of stress in concrete may be adjusted in future study.

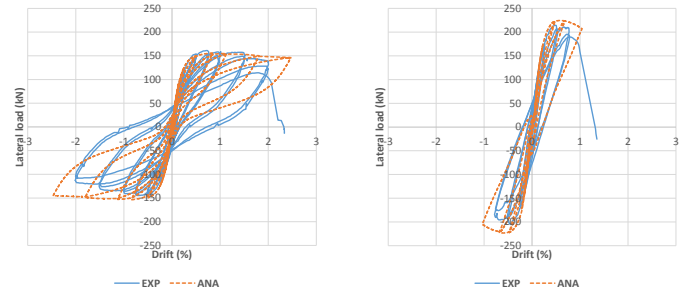


Fig.5 Lateral load-drift relation

Table 1 Compare experimental and analytical characteristic points

Specimen	Approach	Flexural Crack		Yield		Max. load		Ultimate	
		R (%)	Q (kN)	R (%)	Q (kN)	R (%)	Q (kN)	R (%)	Q (kN)
RW20	Exp.	0.14	70.1	0.40	143.9	0.76	161.0	2.03	131.2
	Ana.	0.07	60.0	0.25	125.9	0.84	155.8	1.95	148.4
	Ana./Exp.	0.54	0.86	0.63	0.88	1.11	0.97	0.96	1.13
RW40	Exp.	0.26	169.4	0.09	80.9	0.47	214.4	0.98	167.9
	Ana.	0.14	120.0	0.24	179.1	0.59	224.5	0.94	213.5
	Ana./Exp.	0.53	0.71	2.78	2.21	1.25	1.05	0.96	1.27

VI. CONCLUSIONS

- Axial load ratio of 40% caused low ultimate deformation and sudden concrete crushing as failure mode. Axial load ratio of 20% caused ductile ultimate deformation and spalling of cover concrete followed by core concrete crushing as failure mode. Out-of-plane buckling due to concrete crushing was observed in both specimens when they were loaded beyond their ultimate points.

- Lateral load-drift relation and 4 characteristic points could be simulated by a simple model by cross-section analysis with a good accuracy. The model had assumptions that plastic hinge length equal 0.3 of wall length.

- The model could predict ultimate deformation well with assumption of hoop reinforcement strain of 0.2%.

ACKNOWLEDGMENT

This study was supported by JSPS Grant-in-Aid program (PI: Susumu Kono), the Collaborative Research Project of Materials and Structures Laboratory of Tokyo Institute of Technology and the SOFTech Consortium, Japan.

REFERENCES

- [1] National Earthquake Hazards Reduction Program (NEHRP) (2012): Comparison of U.S. and Chilean Building Code Requirements and Seismic Design Practice 1985–2010. U.S. Department of Commerce National Institute of Standard and Technology.
- [2] Massone LM, Bonelli P, Lagos R, Lüders C, Moehle J, Wallace JW (2012): Seismic Design and Construction Practices for RC Structural Wall Buildings, Earthquake Spectra, 28(S1), S245–S256.
- [3] Chang YY, Deng HZ, Lau DT, Ostovari S, Tsai KC, Khoo HA (2004): A simplified method for nonlinear cyclic analysis of reinforced concrete structures: direct and energy based formulation. 13th World Conference on Earthquake Engineering, Vancouver, Canada.
- [4] Kent R, Park DC (1971), Flexural members with confined concrete. Proceeding of America Society Civil Engineers, vol. 97, 1969–1990.
- [5] Karsan ID and Jirsa JO (1969): Behavior of concrete under compressive loading. Proceeding of America Society Civil Engineers, 95(12), 2543–2564.
- [6] Menegotto M, Pinto PE, (1973): Method of analysis for cyclically loaded RC plane frames including changes in geometry and non-elastic behavior of elements under combined normal force and bending. Preliminary Report IABSE, vol 13, 15–22.
- [7] Beyer K, Dazio A, Priestley MJN (2011): Shear deformation of slender reinforced concrete walls under seismic loading. ACI Structural Journal, 108(2), 167–177.
- [8] Paulay T, Priestley MJN (1992): Seismic Design of Reinforced Concrete and Masonry Buildings. John Wiley & Son, Inc